

LONG TERM BEAM DYNAMICS IN ULTRA-LOW ENERGY STORAGE RINGS

A.I. Papash^{a,b}, A.V. Smirnov^{a,b}, M.R.F. Siggel-King^{c,d} and C.P. Welsch^{c,d}

^aMax Planck Institute for Nuclear Physics, Heidelberg, Germany

^bJoint Institute for Nuclear Research, Dubna, Russia (on leave)

^cUniversity of Liverpool, UK

^dThe Cockcroft Institute for Accelerator Science and Technology, UK

Abstract

Electrostatic storage rings operate at very low energies in the tens of keV range and have proven to be invaluable tools for atomic and molecular physics experiments. However, earlier measurements showed strong limitations in beam intensity, a fast reduction in the stored ion current, as well as significantly reduced beam life time at higher beam intensities and as a function of the ion optical elements used in the respective storage ring. In this contribution, the results from studies with the computer code BETACOOOL into the long term beam dynamics in such storage rings, based on the examples of ELISA are presented.

INTRODUCTION

Due to the mass independence of the electrostatic rigidity, electrostatic storage rings (ESR) at ultra-low energy range are widely used for atomic and molecular physics research [1]. These machines are able to store a wide range of different particles, from light ions to heavy singly charged bio-molecules. Also the next generation Facility for Low energy Antiprotons and Ion Research (FLAIR) at GSI has an ultra-low energy electrostatic storage ring, the USR, as a central facility [2].

Studies into the long term beam dynamics and ion kinetics in such machines are of crucial importance for the performance of the envisaged experiments. For benchmarking purposes, the ELISA electrostatic ring, successfully in operation since the late 90s and dedicated to atomic physics studies [3], has been chosen. In the original ring design spherical deflectors had been used to provide equal focusing in both the horizontal and vertical plane but were later on substituted by cylinder deflectors [4]. Systematic experimental studies showed strong limitations on the maximum storable beam current and reduced beam life time at higher beam intensities. The nature of these effects was not fully understood [5].

Some possible effects that may limit the beam current and life time have been proposed so far [6], including nonlinear fields in the electrostatic elements, parametric resonances due to modulations of the space charge tune shift, as well as coupling between the longitudinal and transverse particle motion. It should be noted that excessive beam losses occurred already at beam

intensities that were too low to be explained by a shift of the betatron tune or parametric resonances [7].

BENCHMARKING OF ELISA DATA

We studied transition processes, i.e. growth rates of beam emittance and momentum spread, as well as equilibrium conditions in ELISA by simulating the rms parameters of the evolution of the ion distribution function with time. For this purpose the BETACOOOL code [8] was used. The program was initially developed to estimate heating and cooling effects in high energy storage rings with electron cooling. It is also possible to implement new physics models in different energy regimes. In this study, the beam parameters summarized in table 1 were used.

BETACOOOL allows choosing and switching between different effects and in this work only heating processes were used: Intra-Beam Scattering (IBS), small angle multiple scattering of the circulating ions on the residual gas atoms and molecules, energy straggling and ion losses on the ring acceptance. It was found quickly that beam losses caused by single large angle scattering are negligible at a vacuum pressure of $2 \cdot 10^{-11}$ Torr, even at such a low beam energy. The limited life time of O^- ions due to the electron detachment by collision with the residual gas as measured by S.P. Møller has been included in the program as an input parameter.

Table 1: BETACOOOL beam parameters of ELISA.

Ion	O^{16}	Mg^{24}
Charge	-1	+1
Ion energy, keV	22	18.4
Initial beam intensities	$5 \cdot 10^5 \div$ $1.6 \cdot 10^7$	$2.7 \cdot 10^7$
Ring circumference, m	7.616	7.616
Initial hor/vert ε, π mm mrad (σ)	1 / 1	0.7/0.35
Initial full ε, π mm mrad (3σ)	6 / 6	4 / 2
Ring acceptance ESD-cyl, π mm mrad	10	10
Ring acceptance ESD-sph, π mm mrad	6	6
Initial RMS momentum spread, $\Delta p/p$	10^{-3}	10^{-4}
Equilibrium momentum spread, $\Delta p/p$	$4 \cdot 10^{-3}$	
Electron detachment life time of O^- , sec	26	--
Life time of O^- at 22 keV, sec	~ 12	

The measured rates of beam intensity decay of a 22 keV O^- beam were reproduced with good accuracy, see Fig. 1. This gave rise to the conclusion that the main

05 Beam Dynamics and Electromagnetic Fields

D02 Non-linear Dynamics - Resonances, Tracking, Higher Order

reasons for beam size growth in a keV storage rings are multiple scattering on the residual gas and Coulomb repulsion of the ions from each other at high intensities, i.e. IBS. As a consequence, the beam is then lost on the ring aperture because of a rather small ring acceptance. The rate of beam losses increases at higher intensities because IBS adds to vacuum losses. The initial shape of the decay curve depends on the beam emittance, the momentum spread and the intensity of the injected beam.

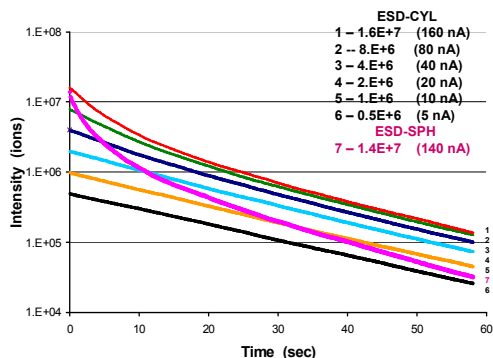


Figure 1: Simulation of beam current decay in ELISA. The intensity of the 22 keV O⁻ beam was varied over a wide range, reflecting earlier measurements [5].

The IBS effect is clearly seen in Fig. 1 as an excessive drop of beam current during the first few seconds when the beam intensity is still high (the green and red curves correspond to initially $8 \cdot 10^6$ and $1.6 \cdot 10^7$ ions, respectively). The long term slope of this loss curve is determined by the ring acceptance and the rate of multiple scattering which is inversely proportional to the vacuum level in the ring. The slope of the decay curve also depends on the life time due to electron detachment for negative ions or electron stripping for positive ions. At very low beam intensities, when IBS is negligible and only scattering on the residual gas is present, the loss rate does not depend on the beam current or details of the ring lattice. That is why all lines in Fig. 1 are almost parallel towards the end of the cycle.

An exception is seen in the pink curve, representing the decay of the beam intensity in ELISA with spherical deflectors. In this case, significantly higher loss rates are caused by the significantly reduced ring acceptance. IBS is also much stronger when the beam density is high and thus in particular in regions where the beam is strongly focused. The IBS rates for ELISA with spherical deflectors are significantly higher than with cylindrical electrodes because of the double focusing effect of the first and the resulting small beam size in both planes.

Earlier studies into non-linear effects in electrostatic storage rings showed that the ELISA ring acceptance is less than 30π mm-mrad and mainly restricted by the sextupole component of the electric field [9]. In this work, the measured equilibrium profile of an 18.6 keV Mg⁺ beam (FWHM=3.43 mm) was compared to BETACOOOL simulations made under the assumption that the transverse beam size is mainly defined by losses on the optical elements of the ring structure, see Fig. 2. The resulting

rms width is equal $\sigma=1.5$ mm and corresponds to a ring acceptance of $A \approx 8\pi$ mm-mrad.

The ring acceptance was then varied as an input parameter in BETACOOOL. Assuming a ring acceptance of $\sim 50 \pi$ mm-mrad, an rms beam size of $\sigma=3$ mm would result, i.e. twice as large as what was measured in the experiment. Also, if the acceptance would be that large the life time of the O⁻ beam in ring should be 24 s which contradicts a measured life time of $\tau \sim 12$ s. Since the long range slope of the decay curve depends on the ring acceptance and is in full agreement with the fact that the ring acceptance with spherical electrodes is much smaller than with cylindrical electrodes, the fast decay in ELISA with spherical deflectors can be explained by a small acceptance $A_{\text{Sph}} \sim 6 \pi$ mm-mrad.

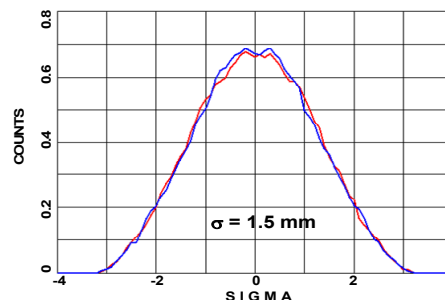


Figure 2: Profile of the Mg⁺ beam corresponds to the ELISA ring acceptance of $A \approx 8\pi$ mm-mrad.

In addition, the fast growth of the momentum spread of a high intensity ($2.7 \cdot 10^7$ ions), low energy (18.3 keV) Mg⁺ beam was reproduced, see Fig. 3. An excellent agreement with experimental results [5] was achieved. It was shown that the fast increase in momentum spread during the first 200 ms is mainly caused by space charge in a beam with a small initial momentum spread, $\Delta p/p=10^{-4}$.

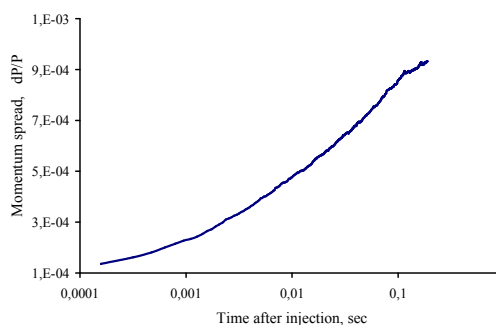


Figure 3: Rms momentum spread of a high intensity Mg⁺ beam as a function of time; BETACOOOL results.

OPERATION WITH INTERNAL TARGET

BETACOOOL was also used to study a coasting beam of ultra-low energy antiprotons circulating in a small recycler ring [10] and its interaction with the He atoms of an ultra-sonic gas jet target, see Table 2.

In addition to IBS, multiple scattering on the residual gas and beam losses on the ring aperture, multiple (small angle) scattering of the antiprotons on the nuclei of the

gas jet target was added, as well as energy losses from excitation and ionization of the He atoms [8,11].

Table 2: BETACOOOL parameters to study the interaction between antiprotons and a supersonic Helium jet target.

Parameter	Value
Antiproton energy range, keV	3 – 30
Ring circumference, m	8.165
Rotation period of pbars in the ring, μ s	11 – 3.5
Initial intensity of antiprotons	5×10^5
Initial rms emittance, π mm mrad (σ)	2
Ring acceptance, π mm mrad	15
Initial momentum spread	10^{-3}
Vacuum pressure (hydrogen), Torr	10^{-11}
Helium target density, cm^{-3}	5×10^{11}
Target length (diameter), mm	1
Hor./vert. beta functions at target, cm	2 / 11
Dispersion at target point, m	0
Ionization cross-section of antiprotons on He atoms, barn [17]	3keV 2×10^7 30keV 6×10^7
Integral of ionization events	3keV $3.5 \cdot 10^3$ 30keV 3.2×10^5
Beam life time, sec	3keV 0.09 30keV 0.82

The antiproton beam is lost on the ring aperture due to the limited acceptance of the recycler. The growth in momentum spread is caused by energy loss fluctuations during interaction with the residual gas and the gas target, see Fig. 4.

The equilibrium beam spot on the target is determined by the ring acceptance and the value of the beta functions at the gas jet location. A low beta lattice was implemented to limit the beam size in the reaction point to ~ 1 mm. Ionization cross-sections of He atoms by low energy antiproton impact were studied and events counted [12]. It was assumed that any ionization event will lead to the loss of an antiproton. This assumption is not evident since the maximum transferable energy is $< 2 \cdot 10^{-3}$ and thus lower than the longitudinal ring acceptance.

The beam life time at 3 keV is limited to 90 ms because of the high multiple scattering rate on the target. In this case, up to 3,500 ionization events can be detected during the first 200 ms. Thereby, more than 99% of this beam will be lost on the ring aperture. With a 30 keV beam, one would measure $\sim 300,000$ ionization events during the first 4 seconds, see Fig. 5.

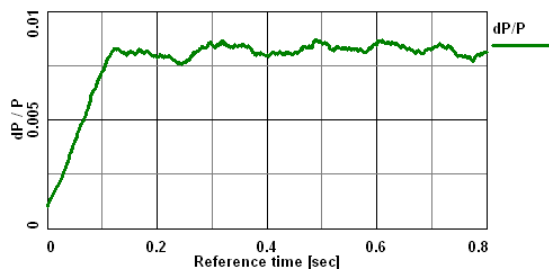


Figure 4: Evolution of the momentum spread of a 3 keV antiproton beam in the presence of a gas jet target.

The beam life time at 30 keV is 0.82 sec. It can be seen that the count rate of such experiment is rather low and might not be better than one event over four-five turns of the antiproton beam in the ring.

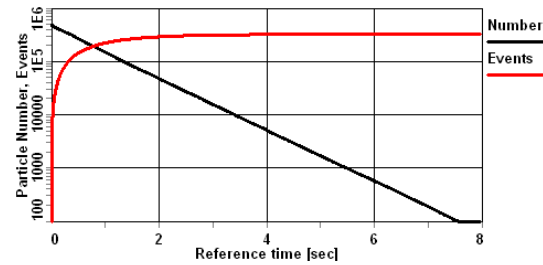


Figure 5: Evolution of the particle number (black) and the integral of ionization events (red) during multiple crossing of 30 keV antiprotons and a Helium jet.

SUMMARY

It was shown how the beam behaviour in keV electrostatic storage rings can be described and what processes lead to beam degradation. Experimental data from ELISA served as a benchmark and was reproduced with very good agreement in BETACOOOL. The results from these studies were used to estimate the event rates of envisaged future collision studies between low energy antiprotons and gas targets in a compact antiproton recycler ring.

REFERENCES

- [1] D. Zajfman et al., Physics with electrostatic rings and traps. *J. Phys. B* **37** (2004)
- [2] C.P. Welsch et al., An ultra-low-energy storage ring at FLAIR. *Nucl. Instr. Meth. A* **546** (2005)
- [3] S.P. Møller, Design and First Operation of the Electrostatic Storage ring ELISA. *Proc. EPAC* (1998)
- [4] S.P. Møller, "Operational experience with the electrostatic storage ring ELISA". *Proc. PAC* (1999)
- [5] S.P. Møller et al., Intensity Limitations of the Storage Ring ELISA. *Proc. EPAC* (2000)
- [6] Y. Senichev, S.P. Møller, Beam Dynamics in Electrostatic Rings. *Proc. EPAC* (2000)
- [7] Y. Senichev, The features of beam dynamics in electrostatic storage rings. FZJ IKP report, Jülich (2000)
- [8] A. Sidorin. BETACOOOL program for simulation of beam dynamics in storage rings. *Nucl. Instr. Meth. A* **558** (2006)
- [9] A.I. Papash, C.P. Welsch, Simulations of space charge effects in low energy electrostatic storage rings. *Proc. IPAC* (2010)
- [10] M.R.F. Siggel-King, A.I. Papash, et al., Electrostatic Low-Energy Antiproton Recycling Ring. *Hyperfine Interactions* **199** (2011)
- [10] F. Hinterberger, D. Prasuhn, Analysis of internal target effects in light ion storage rings. *Nucl. Instr. Meth. A* **279** (1989)
- [11] H. Knudsen, *private communication* (2009)